ChemComm

Accepted Manuscript

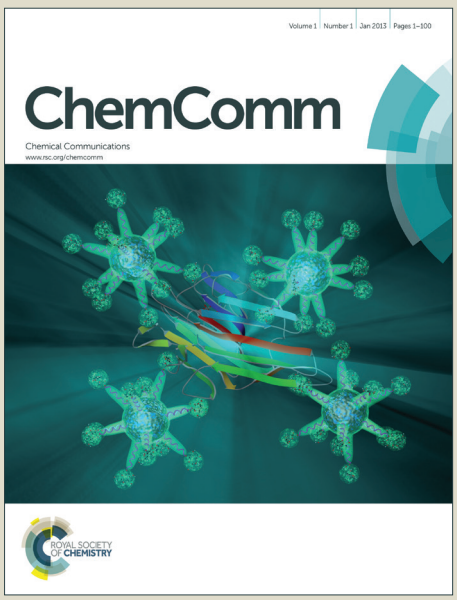

ROYAL SOCIETY OF CHEMISTRY

www.rsc.org/chemcomm

Journal Name

RSCPublishing

COMMUNICATION

A dual functional AEE fluorogen as a mitochondrial-specific bioprobe and an effective photosensitizer for photodynamic therapy

Cite this: DOI: 10.1039/x0xx00000x

Received 00th January 2012,
Accepted 00th January 2012

DOI: 10.1039/x0xx00000x

www.rsc.org/

Engui Zhao,[a,b,†] Haiqin Deng,[a,b,†] Sijie Chen,[a,b] Yuning Hong,[b,d] Chris Wai Tung Leung,[a,b] Jacky Wing Yip Lam,[a,b] Ben Zhong Tang [a,b,c,*]

We report a dual functional aggregation-enhanced emission (AEE) molecule, TPE-IQ, which could target and illuminate mitochondria in both live and fixed cells with superb selectivity and high signal-to-noise ratio. More intriguingly, TPE-IQ can serve as a photosensitizer to generate reactive oxygen species (ROS) in the mitochondria region to induce cell apoptosis.

Fluorescent bioprobes have long been captivating the imagination of researchers. By opening the access of seeing the subcellular structures on site and in time, it enables us to follow the whole biological process in living context.[1] Besides the high temporal and spatial resolution it brings, fluorescent bioprobes enjoy the advantages such as high sensitivity, excellent selectivity, simple operation, in situ workability, etc.[2] On the other hand, photodynamic therapy (PDT) is gaining increasing attention due to its high specificity in eliminating the malignant tumor cells without interfering with normal cells, as compared with chemotherapy.[3,4] Real-time monitoring the morphological changes of certain organelles in cancer cells during the PDT treatment will be of great significance in fundamental and clinical research. In this sense, the combination of bioprobe and photosensitizer will be highly advantageous to facilitate the understanding and innovation of the PDT process.

The most widely used photosensitizers in PDT are porphyrin[5] and phenylthiazinium1[6] derivatives, with few reports on other alternatives. The existing systems, however, are facing the problems such as long incubation and irradiation time, high working concentration and limited specificity.[7–11] To improve the efficiency of a PDT agent, targetability is crucial in the rational design. The nucleus, the command center of the cell, is an excellent intracellular target for PDT. However, as the permeability of nucleus is tightly controlled, limited successes were achieved. On the other hand, due to the critical role of mitochondria in cell apoptosis, a favorable way of cell death, mitochondria have been arising as a promising alternative for target therapy.[12]

Fluorophores with aggregation-induced emission (AIE) have emerged as novel fluorescent materials for biological applications.[13–18] These AIE fluorogens emit weakly when molecularly dissolved, but are highly emissive in aggregated state, which is ideal for biosensing[19–21] and imaging[22–24]. Through molecular engineering, several positively charged AIE fluorophores have been found to stain the mitochondria with superb specificity. Since the fluorescence of bioprobes based on conventional fluorophores will be quenched by increasing the dye concentration, this has forced researchers to utilize them in dilute solutions in nanomolarity, resulting in poor sensitivity and low resistance towards photobleaching.[25–28] In contrast, the AIE mitochondria probes can be used at high concentrations and demonstrates much better photostability. Motivated by these successes, we intend to develop a mitochondria-targeting AIE fluorophore with photosensitivity, which might induce the cell apoptosis effectively while visualizing the whole PDT process.

In this work, we describe an isoquinolinium-based molecule, TPE-IQ, as a dual functional fluorogen – a bioprobe for mitochondrial imaging and novel photosensitizer for PDT. TPE-IQ can be easily synthesized and purified with high yield. It is a cell permeable mitochondria-specific probe with short staining time and fixed cell workability. It is also an effective photosensitizer with low dark toxicity, short incubation and irradiation time and at low working concentration.

The synthetic route to TPE-IQ is shown in Scheme 1. **1** can be facilely synthesized as previous reported.[27,29] Using a multiple component reaction,[30] TPE-IQ was obtained in a one pot reaction in high yield (85%). The structure of TPE-IQ was characterized with NMR and high resolution mass spectrometry (Figure S1-S3), from which satisfactory results corresponding to its structure were obtained.

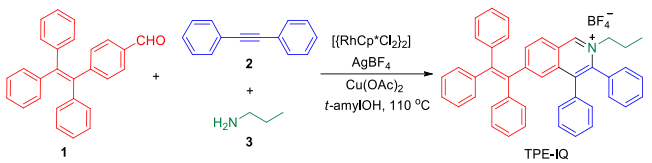

Scheme 1. Synthetic Route to TPE-IQ.

Compared with pure TPE, the absorption maximum of TPE-IQ is red-shifted to around 400 nm (Figure S4). TPE-IQ exhibits the aggregation-enhanced emission (AEE) property. The DMSO solution of TPE-IQ exhibits moderate emission at 502 nm. Adding water to the system leads to the aggregate formation, which enhanced the emission of TPE-IQ (Figure S5). Particle size analysis indicates the formation of aggregates with diameters around 118 nm. (Figure S6)

Before applying TPE-IQ to cell imaging, the cytotoxicity of TPE-IQ was evaluated with lactase dehydrogenase (LDH) cytotoxicity assay (Figure S7). When the cells were incubated with up to 1 μM TPE-IQ for 12 h, cell viability was above 90%, indicative of the good biocompatibility of TPE-IQ. We then investigated the mitochondria targeting ability of TPE-IQ. HeLa cell was co-stained with TPE-IQ (200 nM) and a commercial mitochondria-specific probe, MitoTracker® Red FM (MT) (50 nM), for 15 min. As shown in Figure 1A, the mitochondria are clearly visualized with a very high signal-to-noise ratio. The fluorescence from TPE-IQ overlapped perfectly with MT. The Persons correlation coefficient, which describes the degree of linear dependence between two variables, was 0.98, indicating the good targeting of TPE-IQ towards mitochondria. Since the UV absorption maximum of TPE-IQ is close to the 405 nm, the wavelength of a common violet laser diodes, it is compatible with most of the commercial imaging system settings. As shown in Figure S8, when excited with 405 nm laser, a clear image of the mitochondria with high resolution and fine structural details could be easily obtained.

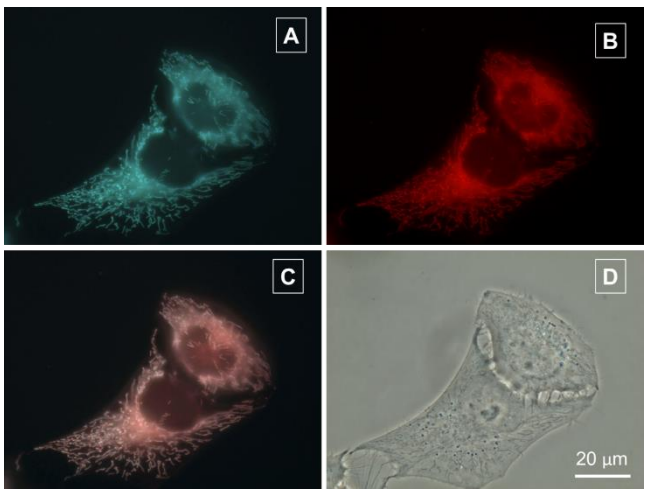

Figure 1. Fluorescent images of HeLa cells stained with (A) TPE-IQ (200 nM) for 15 min and (B) MitoTracker® Red FM (MT, 50 nM) for 15 min. (C) Panels A and B merged. (D) The corresponding bright field image. Excitation wavelength: 330–385 nm (for TPE-IQ) and 540–580 nm (for MT).

The above results show that TPE-IQ can very easily pass through the cell membrane and the staining process can be accomplished in a fast and convenient fashion. When the concentration of TPE-IQ was increased from 200 to 500 nM (Figure S9), a clear image of the mitochondria could be obtained even just with the incubation time of 1 min.

In addition to the fast staining and easy operation in live cell imaging, a versatile fluorescent probe should also be able to stain fixed cells, as fixation is a critical step for sample preservation in biological research. As shown in Figure S10, after cell fixation, TPE-IQ can still target the mitochondria with high selectivity (Figure S10), enabling the mitochondria staining of fixed samples.

More interestingly, TPE-IQ is also a photosensitizer for ROS generation. H2DCF-DA is a commercial ROS probe: its fluorescence at *ca*. 530 nm will be turned on in the presence of any general types of ROS. In the solution of TPE-IQ (10 μM), H2DCF-DA (1 μM) was originally non-fluorescent when excited at 485 nm. When the solution was irradiated with 365 nm UV light for a certain period of time, the emission of H2DCF-DA was turned on and gradually intensified (Figure 2A). After 13 min exposure to UV light, the intensity of H2DCF-DA was 23 time higher than the original emission intensity without UV irradiation. Control experiments showed that, under the same conditions, the pure solution of either TPE-IQ or H2DCF-DA remained non- or weakly emissive upon UV irradiation (Figure S11–S13). These results prove that TPE-IQ can promote the generation of ROS upon UV irradiation.

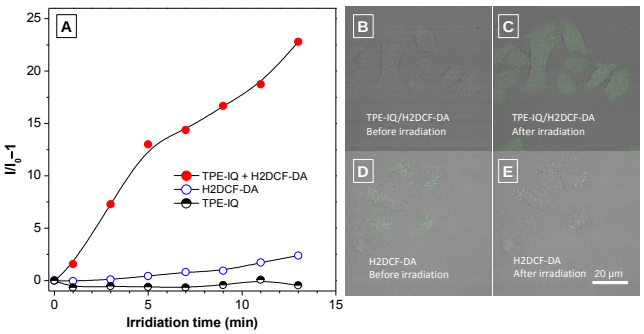

Figure 2. Release of ROS monitored by H2DCF-DA. (A) Change in fluorescent intensity at 534 nm of TPE-IQ, H2DCF-DA, and their mixture in PBS upon UV irradiation (365 nm) for different time. Excitation wavelength: 485 nm. [TPE-IQ] = 10 μM; [H2DCF-DA] = 1 μM. (B-E) Merged bright-field and fluorescence images of Hela cells stained with (B, C) TPE-IQ (1 μM) and H2DCF-DA (1 μM) and (D, E) H2DCF-DA (1 μM) only for 10 min (B, D) before and (C, E) after exposure to 405 nm laser for 2.5 min. Excitation wavelength: 488 nm.

Considering the complexity of biological system, experiment on the detection of TPE-IQ sensitized ROS generation in living cells was then designed and conducted. Cells were incubated with H2DCF-DA (1 μM) and TPE-IQ (1 μM). Before 405 nm laser irradiation, almost no emission from H2DCF-DA could be detected in the cell when excited at 488 nm (Figure 2B). After 405 nm laser irradiation for 2.5 min, the green emission of H2DCF-DA was observed (Figure 2C). For the cells incubated with H2DCF-DA alone, the emission remains faint both before (Figure 2D) and after (Figure 2E) 405 nm laser irradiation. The results indicate that TPE-IQ could serve as sensitizer for ROS generation both in solution and in cells. To gain more insight into the species of the produced ROS, another commercial probe Singlet Oxygen Senor Green (SOSG), specific to singlet oxygen, was utilized (Figure S14): in the mixture of TPE-IQ and SOSG, the emission from SOSG increased progressively with the UV irradiation, suggesting the presence of singlet oxygen in the produced ROS.

When the cells are stained with TPE-IQ, the mitochondrial morphology changes under ROS stress can be induced by UV irradiation and real-time visualized under a fluorescent microscopy. As shown in Figure 3, with the gradually increased irradiation time, the structure of mitochondria changed from long tubular like, to disconnected reticulum and eventually to small and dispersed fragments. The swelling of mitochondria implies the depolarization of the mitochondria membrane potential.[31] The specific targeting of TPE-IQ to mitochondria enables the ROS generation in the mitochondrial region to trigger the mitochondrial-mediated apoptotic pathway, in which the mitochondrial protein, such as cytochromo *c*, will be released to the cytosol, to activate the caspase and initiate the cell apoptosis.[32,33]

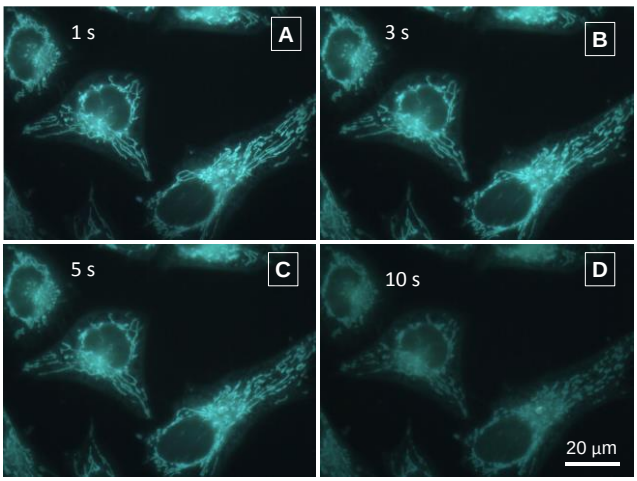

Figure 3. Fluorescent images of HeLa cells stained with TPE-IQ (500 nM) for 10 min and exposed to UV irradiation with different duration: (A) 1 s; (B) 3 s; (C) 5 s; (D) 10 s. Excitation wavelength: 330–385 nm.

The effect of TPE-IQ sensitized ROS generation on cell viability was then evaluated. In the experimental group, cells were treated with different concentrations of TPE-IQ for 15 min and then exposed to UV irradiation for 2 min, followed by furthering incubation in dark for 12 h. As a control experiment, the cells were treated with the same concentrations of TPE-IQ but without irradiation.

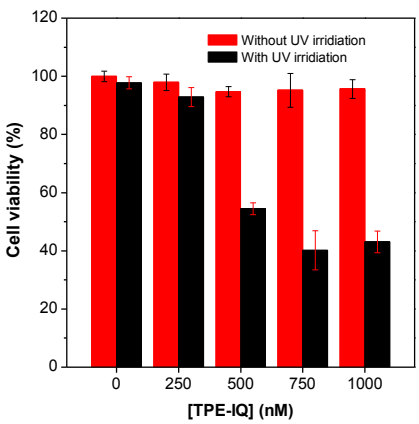

Figure 4. Cell viability assessed by the LDH method. After incubation with TPE-IQ for 15 min, the cells were treated without/ with UV irradiation for 2 min, followed by further incubation with TPE-IQ for 12 h in dark.

Cytotoxicity was then evaluated by LDH method. The result suggested that without UV irradiation, TPE-IQ posed negligible effect on the cell viability even when the cells were incubated with 1 μM of TPE-IQ for 12 h (Figure 4). With UV irradiation, the cell viability decreased significantly to around 40% with 1 μM TPE-IQ. Note that in the absence of TPE-IQ, UV treatment for the same period of time would not affect the cell viability significantly with more than 96% of cells viable. Meanwhile, in the imaging concentration of 200 nM, TPE-IQ does not have significant cytotoxicity even under UV irradiation.

In LDH assay, cytotoxicity is evaluated by the LDH released from the damaged plasma membrane of the dead cells. However, the membranes of cells undergoing apoptosis may remain relatively integrate and thus this method may underestimate the actual cytotoxicity of the analytes. To further examine the cytotoxicity, propidium iodide (PI) staining was applied. PI is a cell impermeable dye, which stains dead cells or late apoptotic cells with damaged membrane only. The cells stained with TPE-IQ are healthy with normal morphology (Figure 5A). In the fluorescence channel of the imaging field, no emission from PI can be observed (Figure 5C). After UV irradiation, the TPE-IQ stained cells shrank and detached from the substrate, suggesting the unhealthy state of these cells (Figure 5B). Red emission from PI was observed in all the cells, indicating these cells are effectively killed by the TPE-IQ sensitized ROS generation (Figure 5D). Control groups of unstained cells with or without UV treatment cannot be stained with PI (Figure S15), proving the vital role of TPE-IQ in causing the cell death.

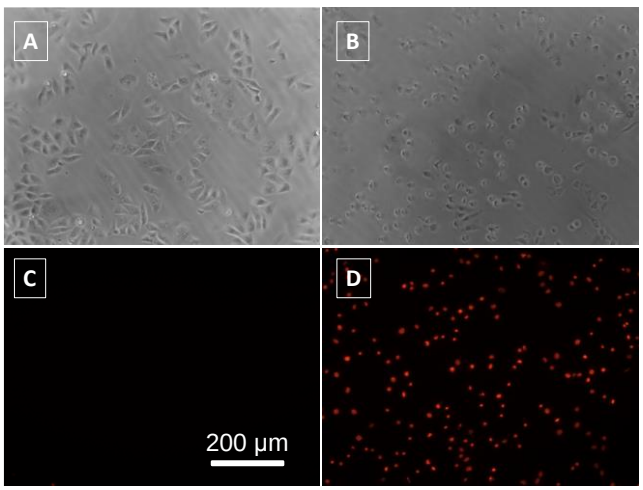

Figure 5. (A, B) Bright field and (C, D) fluorescence images of PI stained (1.5 μM, 10 min) Hela cells. After incubation with TPE-IQ for 15 min, the cells were treated (A, C) without/ (B, D) with UV irradiation for 2 min, followed by further incubation with TPE-IQ for 12 h in dark.

To sum up, in this work, we report a new AEE molecule, TPE-IQ, with dual functionalities: mitochondria-specific imaging and potential application in PDT. As a fluorescent probe, TPE-IQ can stain the mitochondria in live and fixed cells with high selectivity and sensitivity. The staining process in live cells can be achieved by incubating with low concentration of TPE-IQ within 1 minute. As a photo sensitizer, TPE-IQ could generate ROS upon UV irradiation. Such process induces the cell apoptosis effectively and could potentially be applied to PDT. Thanks to its mitochondrial targeting ability, the PDT process could take place in an efficient fashion with short incubation and irradiation time at low working concentration.

Taking advantages of these two functionalities, one can monitor the mitochondria morphology changes during the apoptosis, which may of great implication in revealing details in the apoptosis-associated biological process and designing new strategies of PDT for cancer treatment.

This work was partially supported by National Basic Research Program of China (973 Program; 2013CB834701), the Research Grants Council of Hong Kong (604913, 604711, 6602212, 16301614 and N_HKUST620/11), and the University Grants Committee of Hong Kong (AoE/P-03/08). B.Z.T. thanks the support from Guangdong Innovative Research Team Program (201101C0105067115).

Notes and references

[a] HKUST Shenzhen Research Institute, No. 9 Yuexing 1st RD, South Area, Hi-tech Park Nanshan, Shenzhen 518057, China. Email: tangbenz@ust.hk.
[b] Division of Biomedical Engineering, Department of Chemistry, Institute for Advanced Study, Division of Life Science, Institute of Molecular Functional Materials and State Key Laboratory of Molecular Neuroscience, The Hong Kong University of Science & Technology (HKUST), Clear Water Bay, Kowloon, Hong Kong, China
[c] Guangdong Innovative Research Team, SCUT-HKUST Joint Research Laboratory, State Key Laboratory of Luminescent Materials and Devices, South China University of Technology (SCUT), Guangzhou 510640, China
[d] School of Chemistry, The University of Melbourne, Parkville, VIC 3010, Australia
† E.Z. and H.D. contributed equally to this work.

Electronic Supplementary Information (ESI) available: ^{1}H NMR, ^{13}C NMR, and HRMS spectrum of TPE-IQ, UV and PL spectrum, cytotoxicity evaluation, particle size analysis, LCSM image, fluorescence images of live and fixed HeLa cell, PL spectrum of H2DCF-DA with/without TPE-IQ, singlet oxygen generation evaluated with SOSG, and images of HeLa cell with/without UV irradiation are in the supporting information. See DOI: 10.1039/c000000x/.

1 I. L. Medintz, H. T. Uyeda, E. R. Goldman, and H. Mattoussi, *Nat. Mater.*, 2005, **4**, 435.
2 M. J. Rust, M. Bates, and X. Zhuang, *Nat. Methods*, 2006, **3**, 793.
3 J. P. Celli, B. Q. Spring, I. Rizvi, C. L. Evans, K. S. Samkoe, S. Verma, B. W. Pogue, and T. Hasan, *Chem. Rev.*, 2010, **110**, 2795.
4 M. Ethirajan, Y. Chen, P. Joshi, and R. K. Pandey, *Chem. Soc. Rev.*, 2011, **40**, 340.
5 E. S. Nyman and P. H. Hynninen, *J. Photochem. Photobiol. B Biol.*, 2004, **73**, 1.
6 M. Wainwright, *Photodiagnosis Photodyn. Ther.*, 2005, **2**, 263.
7 T.-I. Peng, C.-J. Chang, M.-J. Guo, Y.-H. Wang, J.-S. Yu, H.-Y. Wu, and M.-J. Jou, *Ann. N. Y. Acad. Sci.*, 2005, **1042**, 419.
8 T.-I. Peng, C.-J. Chang, S.-B. Jou, C.-M. Yang, and M.-J. Jou, *Opt. Quantum Electron.*, 2006, **37**, 1377.
9 P. Prasad, I. Khan, P. Kondaiah, and A. R. Chakravarty, *Chemistry*, 2013, **19**, 17445.
10 Y. Chen, A. Gryshuk, S. Achilefu, T. Ohulchansky, W. Potter, T. Zhong, J. Morgan, B. Chance, P. N. Prasad, B. W. Henderson, A. Oseroff, and R. K. Pandey, *Bioconjug. Chem.*, 2005, **16**, 1264.
11 J. Saczko, M. Mazurkiewicz, a Chwiłkowska, J. Kulbacka, G. Kramer, M. Ługowski, M. Snietura, and T. Banaś, *Folia Biol.* , 2007, **53**, 7.
12 J. S. Modica-Napolitano and J. R. Aprille, *Adv. Drug Deliv. Rev.*, 2001, **49**, 63.
13 Y. Hong, J. W. Y. Lam, and B. Z. Tang, *Chem. Commun.* , 2009, 4332.
14 Y. Hong, J. W. Y. Lam, and B. Z. Tang, *Chem. Soc. Rev.*, 2011, **40**, 5361.
15 Y. Yuan, G. Feng, W. Qin, B. Z. Tang, and B. Liu, *Chem. Commun.* , 2014, **50**, 8757.
16 F. Hu, Y. Huang, G. Zhang, R. Zhao, H. Yang, and D. Zhang, *Anal. Chem.*, 2014, **86**, 7987.
17 C.-C. Chang, M.-C. Hsieh, J.-C. Lin, and T.-C. Chang, *Biomaterials*, 2012, **33**, 897.
18 M.-C. Hsieh, C.-H. Chien, C.-C. Chang, and T.-C. Chang, *J. Mater. Chem. B*, 2013, **1**, 2350
19 X. Li, S. Zhu, S. Yao, Z. Liu, B. Xu, B. Yang, and W. Tian, *Anal. Chem.*, 2014, **86**, 298.
20 X. Xu, J. Li, Q. Li, J. Huang, Y. Dong, Y. Hong, J. Yan, J. Qin, Z. Li, and B. Z. Tang, *Chem. Eur. J.*, 2012, **18**, 7278.
21 M. Wang, G. Zhang, D. Zhang, D. Zhu, and B. Z. Tang, *J. Mater. Chem.*, 2010, **20**, 1858.
22 E. Zhao, Y. Hong, S. Chen, C. W. T. Leung, C. Y. K. Chan, R. T. K. Kwok, J. W. Y. Lam, and B. Z. Tang, *Adv. Healthc. Mater.*, 2014, **3**, 88.
23 Y. Yuan, R. T. K. Kwok, G. Feng, J. Liang, J. Geng, B. Z. Tang, and B. Liu, *Chem. Commun.* , 2014, **50**, 295.
24 Y. Huang, F. Hu, R. Zhao, G. Zhang, H. Yang, and D. Zhang, *Chem. Eur. J.*, 2014, **20**, 158.
25 C. W. T. Leung, Y. Hong, S. Chen, E. Zhao, J. W. Y. Lam, and B. Z. Tang, *J. Am. Chem. Soc.*, 2013, **135**, 62.
26 W. Chen, D. Zhang, W. Gong, Y. Lin, and G. Ning, *Spectrochim. Acta. A. Mol. Biomol. Spectrosc.*, 2013, **110**, 471.
27 N. Zhao, M. Li, Y. Yan, J. W. Y. Lam, Y. L. Zhang, Y. S. Zhao, K. S. Wong, and B. Z. Tang, *J. Mater. Chem. C*, 2013, **1**, 4640.
28 Y. Chen, L. Qiao, B. Yu, G. Li, C. Liu, L. Ji, and H. Chao, *Chem. Commun.* , 2013, **49**, 11095.
29 R. Hu, J. L. Maldonado, M. Rodriguez, C. Deng, C. K. W. Jim, J. W. Y. Lam, M. M. F. Yuen, G. Ramos-Ortiz, and B. Z. Tang, *J. Mater. Chem.*, 2012, **22**, 232.
30 J. Jayakumar, K. Parthasarathy, and C.-H. Cheng, *Angew. Chem. Int. Ed.* , 2012, **51**, 197.
31 J. D. Ly, D. R. Grubb, and a Lawen, *Apoptosis*, 2003, **8**, 115.
32 M. Karbowski and R. J. Youle, *Cell Death Differ.*, 2003, **10**, 870.
33 D.-F. Suen, K. L. Norris, and R. J. Youle, *Genes Dev.*, 2008, **22**, 1577.

